Journal of Sound and Vibration (1997) **205**(5), 593–615

THE DYNAMICS OF A NON-LINEAR SYSTEM SIMULATING LIQUID SLOSHING IMPACT IN MOVING STRUCTURES

V. N. Pilipchuk and R. A. Ibrahim

Department of Mechanical Engineering, *Wayne State University*, *Detroit*, *Michigan* 48202, *U.S.A.*

(*Received* 3 *September* 1996, *and in final form* 10 *March* 1997)

In this paper the non-linear modal interaction is examined betwen liquid hydrodynamic impact and an elastic support structure. The liquid impact is modelled based on a phenomenological concept by introducing a power non-linearity with a higher exponent. A special saw-tooth time transformation (STTT) technique is used analytically to describe the in-phase and out-of-phase strongly non-linear periodic regimes. Based on explicit forms of analytical solutions, all basic characteristics of the non-linear free and forced response regimes, such as the time history, the amplitude–frequency dependence and the non-linear parametric resonance curves, are estimated. The response behavior reveals that a high frequency out-of-phase non-linear mode takes place with a relatively small tank amplitude, and is more stable than the in-phase oscillation mode under small perturbations. The in-phase mode has relatively large tank amplitudes and does not preserve its symmetry under periodic parametric excitation.

1. INTRODUCTION

Liquid containers constitute major components in a number of dynamical systems, such as aerospace vehicles, road tankers and liquefied natural gas carriers. Liquid sloshing in a moving container creates a broad class of problems of practical safety, including tank trucks on highways, liquid tank cars on railroads and liquid cargo in ocean-going vessels. Gasoline and other flammable liquid tankers are prone to rollover accidents when entering and exiting highways.

Analytical techniques for predicting large amplitude sloshing are not fully developed. Such loads are extremely important in designing the support structure and internal components of a vehicle's tank. In addition, much of the sloshing technology developed for space applications [1] is not applicable to road tankers, because emphasis has been placed on frequencies and total forces as they relate to control system requirements and, therefore, the effects of local peak impact pressure on structural requirements have not been studied to any extent. Furthermore, the excitation amplitudes considered in space applications are too small for road vehicle simulation.

The study of liquid sloshing dynamics within a moving vehicle involves different types of modelling and analysis. Gustafson and Gustafson [2] presented an extensive survey pertaining to the overturning problem of heavy vehicles. Isermann [3] computed the overturning limit for some tank semi-trailers during steady state cornering. Bauer [4] provided an analytical treatment for different container geometries partially filled with liquid. The analysis includes estimates for liquid natural frequencies, forces and moments. Slibar and Troger [5, 6] analyzed the lateral wheel load transfer ratio of a tractor

0022–460X/97/350593 + 23 $25.00/0/sv971034

semi-trailer system. The forces and moments from the liquid load for harmonic oscillation steering were introduced via a mechanical model approach. Each compartment includes one rigid and one moving mass. The moving masses are restrained by linear springs and dashpots. It is speculated that liquid-carrying vehicles have more accidents than other vehicles, in part because of the large movement of the liquid cargo, with its attendant forces and moments. Liquid sloshing during a highway maneuver can lead to lateral and roll instabilities, decreased controllability/maneuverability, and increased stress on tank structures. The influence of large amplitude liquid sloshing on the overturning and skidding stability of road tankers is very serious during dynamic maneuvers. Strandberg [7] conducted experimental investigations to measure liquid sloshing forces in laterally oscillating model tanks, with or without baffles and cross-walls. The effects of liquid forces on overturning and skidding tendencies were evaluated from simplified vehicle models (no roll, no yaw) in a hybrid computer.

The problem of liquid sloshing involves the estimation of hydrodynamic pressure distribution forces and moments. These hydrodynamic forces may have a strong influence on the dynamics of the elastic structure carrying liquid containers. The non-linear interaction of liquid sloshing with the dynamics of the elastic supporting structure subjected to vertical sinusoidal ground motion was examined in the neighborhood of internal resonance by Ibrahim and Barr [8, 9], Ibrahim [10] and Ibrahim *et al*. [11]. In the neighborhood of internal resonance conditions the system experienced complex response characteristics such as jump phenomena, multiple solutions and energy exchange. Non-stationary responses with cases including violent system motion, which can lead to the collapse of the system, were observed experimentally in the neighborhood of multiple internal resonances. Liquid–structure interaction under horizontal periodic motion was studied by Ibrahim and Li [12]. More realistic cases, such as simultaneous random horizontal and vertical ground excitations, were examined by Soundararajan and Ibrahim [13] using the theory of weakly non-linear differential equations.

Sloshing phenomena are governed by liquid fill depths. For the case of low fill depth, the liquid free surface motion is characterized by the formation of hydraulic jumps and traveling waves for excitation periods around resonance. At higher fill depths, large standing waves are usually formed in the resonant frequency range. When hydraulic jumps or traveling waves are present, extremely high impact pressures can occur on the tank walls. Typical pressure traces recorded under this sloshing condition were reported by Cox *et al*. [14]. Impact pressures can also occur on the tank top when tanks are filled to the higher fill depth, and the pressure variation is neither harmonic nor periodic, since the magnitude and duration of the pressure peaks vary from cycle to cycle even though the tank is experiencing harmonic oscillation.

It is clear that liquid pressure impacts are one of the sources of non-linearity in a liquid tank supported on an elastic structure. The addition of the impact to a harmonic oscillator immediately results in a strongly non-linear system. This is in contrast to most non-linear systems that have been studied, in which the non-linearity is assumed to be small and quasi-linear perturbation techniques can be applied. In this case the dynamicist should utilize the techniques developed for the theory of vibro-impact of rigid body systems [15–21]. In this paper, the problem of the fluid hydrodynamic sloshing impact with the supported structure will be examined using the technique of saw-tooth time transformations (STTT). Note that a transformation of co-ordinates by means of non-smooth functions which allows us to eliminate impact constraints was introduced by Zhuravlev [22]. This transformation deals with the system co-ordinates and can be directly applied for cases of absolutely rigid constrains.

In the present paper, the hydro-impact phenomenon will be modelled using a phenomenological power non-linearity with high exponent. As a result, the model does not include absolute rigid constrains and thus will be considered using the STTT technique. The physical and mathematical principals of the STTT have been formulated by Pilipchuk [23–25] and are documented in a research monograph by Vakakis *et al*. [26]. This technique is based on a special transformation of time and gives explicit form analytical solutions for the power non-linearities which are considered in the present work. To the authors' knowledge, this is the first attempt to model the liquid sloshing pressure impact by a strongly non-linear system, the parameters of which can be obtained by experimental measurements. This task is currently being considered by the authors.

2. LIQUID SLOSHING MODELING

Generally, the liquid hydrodynamic pressure in moving rigid containers is comprised of two distinct components. One component is directly proportional to the acceleration of the tank. This component is caused by part of the fluid moving in unison with the tank. The second component is known as "convective" pressure and experiences sloshing at the free surface. Accordingly, three dynamic regimes are possible, as demonstrated in Figure 1:

(1) Small oscillations in which the fluid free surface remains planar without rotation (see Figure 1(a)). This regime can be described by a linear equation for the first asymmetric sloshing mode which is equivalent to a pendulum describing small oscillations such that $\sin\theta \simeq \theta$.

(2) Relatively large amplitude oscillations in which the liquid free surface experiences both non-planar and rotational motions (see Figure 1(b)). This regime is described by a differential equation with weak non-linearity and can be analyzed using the standard

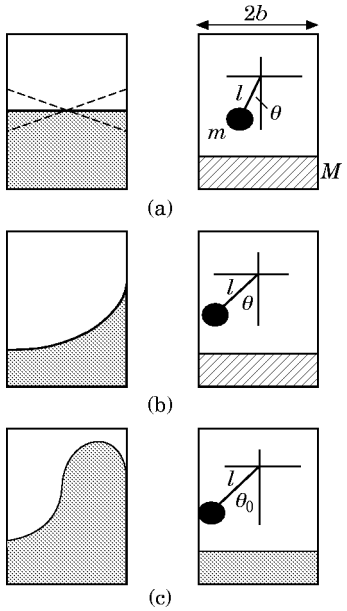

Figure 1. Regimes of liquid free surface motion and their modelling: (a) linear modelling, describing planar motion, $l = b$, $\sin\theta \approx \theta$; (b) weakly non-linear modelling, describing non-planar motion, $l \leqslant b$, $\sin\theta \approx \theta - \theta^3/3!$; (c) hydrodynamic impact pressure, $l > b$.

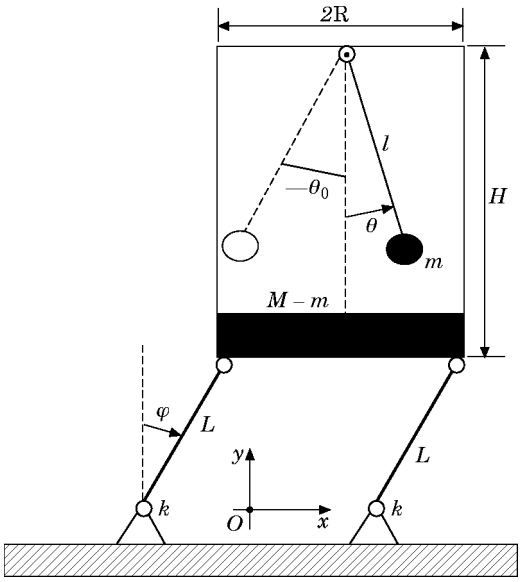

Figure 2. A schematic diagram of the model.

perturbation techniques. The equivalent mechanical model is the simple pendulum such that $\sin\theta \simeq \theta - \theta^3/3!$.

(3) Strongly non-linear motion, where the non-linearity is mainly due to rapid velocity changes associated with hydrodynamic pressure impacts of the liquid portion close the the free surface (see Figure 1(c)). The velocity changes of the liquid free surface are usually treated as being instantaneous (velocity jumps) and they lead to various strongly non-linear features of the system behavior. This regime can be modelled by a pendulum describing impacts with the tank walls. This is the case of the present work.

The mathematical modelling of liquid containers supported on elastic structures can be developed by considering a liquid container supported by four massless rods of length L, which are restrained by four torsional springs k at the base as shown in Figure 2. Let M be the total mass of the container including liquid, and m be the equivalent sloshing mass of the first asymmetric mode of the liquid. The fluid free surface is modelled as a pendulum of length l. The pendulum can reach the walls of the tank if its angle with the vertical axis is $\theta = \pm\theta_0$. Considering the pendulum and the tank walls as rigid bodies, one must introduce the constraint that $|\theta| \leqslant \theta_0$. This type of modelling is similar to the one used by Shaw and Shaw [27], who represented the impact by the momentum equation together with the definition of the coefficient of restitution. They also assumed the collision between the pendulum mass and the tank wall as a discontinuous process. From the point of view of analytical techniques in non-linear mechanics, such constraints essentially complicate the analysis, because one must match solutions at points of interaction $\{t:\theta(t) = \pm\theta_0\}$, which are *a priori* unknown. Hence there is a reason to avoid operations with constraints. As mentioned in the introduction, a sufficiently simple non-smooth transformation of co-ordinates leading to the exclusion of constraints was proposed in reference [22]. However, the simplest method does not introduce the constraints at all. Indeed, one can phenomenologically describe the interaction between the pendulum and the tank walls with a special potential field of interaction, which is very weak in the region $|\theta| < \theta_0$, but becomes fast growing in the neighborhood of the points $\theta = \pm\theta_0$. For example, the

desirable properties of the potential field can be provided by means of the following function of the potential energy,

$$\Pi_i(\theta) = \frac{b\theta_0}{2n}\left(\frac{\theta}{\theta_0}\right)^{2n}, \tag{1}$$

where $n \gg 1$ is a positive integer, and b is a positive constant parameter. The force of interaction is

$$F_i = \frac{\mathrm{d}\Pi_i(\theta)}{\mathrm{d}\theta} = b\left(\frac{\theta}{\theta_0}\right)^{2n-1}, \tag{2}$$

which is demonstrated in Figure 3 for different values of n. One has a limit of absolutely rigid bodies interaction, if $n \to \infty$. For this case the potential energy (1) takes the square well form. If the exponent $2n - 1$ is large and finite, then the interaction field is not absolutely localized at the points $\theta = \pm\theta_0$. This means that the tank walls and the pendulum mass are not absolutely rigid, but admit a small deformation about the points of contact $\theta = \pm\theta_0$. Because of this, a finite value of n seems more realistic than the rigid body limit; yet the approach considered includes the rigid body limit as a particular case.

Suppose that the energy dissipation of the pendulum basically results from the pendulum interaction with the container walls. This means that the dissipation is spatially localized around the points $\theta = \pm\theta_0$. The localized dissipative force will be approximated by the

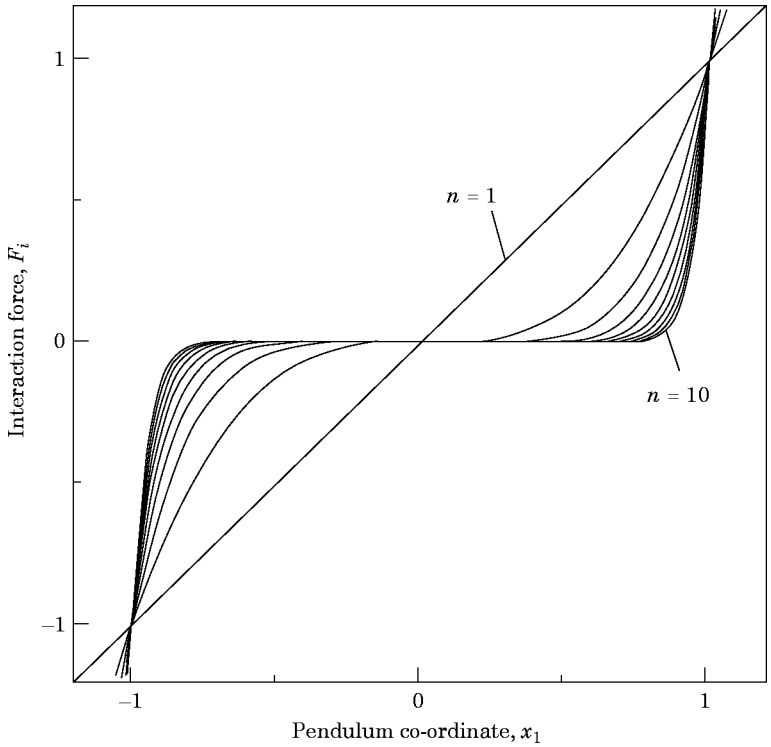

Figure 3. The force of impact between the tank and the pendulum for different exponents of the power function of $x_1 = \theta/\theta_0$.

expression

$$F_d = d\left(\frac{\theta}{\theta_0}\right)^{2p} \dot{\theta}, \tag{3}$$

where d is a constant coefficient, $p \gg 1$ is a positive integer (generally, $p \neq n$), and a dot denotes differentiation with respect to time t.

This impact representation was described by means of power functions by Hunt and Grossley [28]. They used local co-ordinates about the point of interaction, and thus the exponents of the power functions are not large numbers compared with 1. The representation (2) for impact interactions was also used in reference [29].

With reference to Figure 2, the Cartesian co-ordinates of the pendulum and the container mass centers are $x_p = L \sin\varphi + l \sin\theta$, $y_p = L \cos\varphi - l \cos\theta + H$ and $x_c = L \sin\varphi$, $y_c = L \cos\varphi$, respectively. The potential energy of the system can be written as

$$\Pi = \frac{k\varphi^2}{2} + (M-m) + gy_c + mgy_p + \frac{b\theta_0}{2n}\left(\frac{\theta}{\theta_0}\right)^{2n} + \text{constant}$$

$$= \frac{k\varphi^2}{2} + (M-m)gL\cos\varphi + mg(L\cos\varphi - l\cos\theta) + \frac{b\theta_0}{2n}\left(\frac{\theta}{\theta_0}\right)^{2n} + \text{constant}, \tag{4}$$

where the constant is an additive constant that will have no influence on the equation of motion.

The kinetic energy is

$$T = \frac{m}{2}(\dot{x}_p^2 + \dot{y}_p^2) + \frac{M-m}{2}(\dot{x}_c^2 + \dot{y}_c^2)$$

$$= \frac{M-m}{2}L^2\dot{\varphi}^2 + \frac{m}{2}[L^2\dot{\varphi}^2 + 2lL\cos(\varphi+\theta)\dot{\varphi}\dot{\theta} + l^2\dot{\theta}^2]. \tag{5}$$

Introducing the linear law of dissipation for the container and taking the non-linear dissipation (3) for the pendulum, the elementary work done by the dissipative force can be written as

$$\mathrm{d}W_d = -c\dot{\varphi}\,\mathrm{d}\varphi - d\left(\frac{\theta}{\theta_0}\right)^{2p}\dot{\theta}\,\mathrm{d}\theta,$$

where the minus sign means that the energy is taken out from the system, and c is a linear viscous damping coefficient.

Let $F_x(t)$ and $F_y(t)$ be the components of an external force per unit mass along the x- and y-axes respectively. Elementary work done by the external force is

$$\mathrm{d}W_e = m[F_x(t)\,\mathrm{d}x_p + F_y(t)\,\mathrm{d}y_p] + (M-m)[F_x(t)\,\mathrm{d}x_c + F_y(t)\,\mathrm{d}y_c]$$

$$= ML[F_x(t)\cos\varphi - F_y(t)\sin\varphi]\,\mathrm{d}\varphi + ml[F_x(t)\cos\theta + F_y(t)\sin\theta]\,\mathrm{d}\theta.$$

The Lagrangian equations of motion are

$$\frac{\mathrm{d}}{\mathrm{d}t}\frac{\partial L}{\partial \dot{\theta}} = \frac{\partial L}{\partial \theta} = \frac{\partial W_d}{\partial \theta} + \frac{\partial W_e}{\partial \theta}, \qquad \frac{\mathrm{d}}{\mathrm{d}t}\frac{\partial L}{\partial \dot{\varphi}} - \frac{\partial L}{\partial \varphi} = \frac{\partial W_d}{\partial \varphi} + \frac{\partial W_e}{\partial \varphi}, \tag{6, 7}$$

where $L = T - \Pi$ is the Lagrangian function.

Applying equations (6) and (7) with respect to the angle co-ordinates θ and φ, the following equations of motion are obtained:

$$l^2 m\ddot{\theta} + lLm\cos(\theta+\varphi)\ddot{\varphi} - lLm\sin(\theta+\varphi)\dot{\varphi}^2 + lm[g - F_y(t)]\sin\theta + d\left(\frac{\theta}{\theta_0}\right)^{2p}\dot{\theta} + b\left(\frac{\theta}{\theta_0}\right)^{2n-1} = lmF_x(t)\cos\theta, \tag{8}$$

$$lLm\cos(\theta+\varphi)\ddot{\theta} + L^2 M\ddot{\varphi} - lLm\sin(\theta+\varphi)\dot{\theta}^2 + c\dot{\varphi} + k\varphi - LM[g - F_y(t)]\sin\varphi = LMF_x(t)\cos\varphi. \tag{9}$$

These equations include geometrical non-linearities (inertia and stiffness) and impact non-linearities due to the phenomenological expressions (2) and (3). The stiffness geometrical non-linearities are expressed by the trigonometrical functions. For a small magnitude of the angle θ_0, i.e., $\theta_0 = \varepsilon \ll \pi/2$, the impact will be observed in a small region of the angle co-ordinate, where $\theta \sim \varepsilon$. In this region the relationships $\sin\theta = \theta + O(\varepsilon^3)$ and $\cos\theta = 1 + O(\varepsilon^2)$ hold. Thus the geometrical non-linear terms are of orders $O(\varepsilon^2)$ and $O(\varepsilon^3)$, and at the same time the "impact" non-linearity is $(\theta/\theta_0)^{2n-1} = O(1)$. If higher order terms are retained, then the resulting geometrical non-linearities may cause the occurrence of internal resonance. The influence of internal resonance in the presence of impact nonlineary will be treated in a separate study.

It follows that one can keep the "impact" non-linear terms but linearize the rest of the terms in equations (8) and (9). As a result, one obtains

$$l^2 m\ddot{\theta} + lLm\ddot{\varphi} + lm[g - F_y(t)]\theta + d\left(\frac{\theta}{\theta_0}\right)^{2p}\dot{\theta} + b\left(\frac{\theta}{\theta_0}\right)^{2n-1} - lmF_x(t), \tag{10}$$

$$lLm\ddot{\theta} + L^2 M\ddot{\varphi} - LM[g - F_y(t)]\varphi + c\dot{\varphi} + k\varphi = LMF_x(t). \tag{11}$$

Let us measure the angles and time in a scale of the free pendulum oscillations with amplitude θ_0 (when the tank is stationary) by introducing the following dimensionless variables:

$$x_1 = \theta/\theta_0, \qquad x_2 = \varphi/\theta_0, \qquad \bar{t} = \sqrt{\frac{g}{l}}t, \qquad \mu = m/M, \qquad \lambda = l/L, \tag{12}$$

$$2\delta_1 = \frac{d}{Lmg}\sqrt{\frac{g}{l}}, \qquad 2\delta_2 = \frac{c}{Lmg}\sqrt{\frac{g}{l}}, \qquad \beta = \frac{b}{Lmg\theta_0},$$

$$f_x(\bar{t}) = \frac{F_x(t)}{g\theta_0}, \qquad f_y(\bar{t}) = \frac{F_y(t)}{g}, \qquad \nu = \frac{\omega_L}{\omega_l} = \sqrt{\lambda\left(\frac{k}{MLg} - 1\right)},$$

$$\omega_L^2 = \frac{k - LMg}{ML^2}, \qquad \omega_l^2 = \frac{g}{l}. \tag{13}$$

The last parameter ν is impotent for future analysis and denotes the ratio of two local frequencies; i.e. ω_L is frequency of the tank in the absence of the pendulum motion, and

ω_l is the frequency of the pendulum if the tank is standstill. The frequency ω_l is equivalent to the fluid first antisymmetric sloshing mode and depends on the tank geometry and fluid depth (see reference [1] for closed form expressions of liquid natural frequencies for different tank geometries).

Taking into account the notations listed in equations (12) and (13) gives the following dimensionless equations of motion in the matrix form:

$$\mathbf{B}\frac{\mathrm{d}^2\mathbf{x}}{\mathrm{d}\bar{t}^2} + 2\mathbf{D}(\mathbf{x})\frac{\mathrm{d}\mathbf{x}}{\mathrm{d}\bar{t}} + [\mathbf{K} + \mathbf{P}(\bar{t})]\mathbf{x} + \beta\mathbf{N}(\mathbf{x}) = \mathbf{Q}(\bar{t}), \tag{14}$$

where $\mathbf{x} = (x_1 \quad x_2)^{\mathrm{T}}$ and

$$\mathbf{B} = \begin{pmatrix} \lambda & 1 \\ 1 & 1/(\lambda\mu) \end{pmatrix}, \qquad \mathbf{D}(\mathbf{x}) = \begin{pmatrix} \delta_1 x_1^{2p} & 0 \\ 0 & \delta_2 \end{pmatrix}, \qquad \mathbf{K} = \begin{pmatrix} \lambda & 0 \\ 0 & v^2/(\lambda\mu) \end{pmatrix},$$

$$\mathbf{P}(\bar{t}) = f_y(\bar{t})\begin{pmatrix} -\lambda & 0 \\ 0 & 1/\mu \end{pmatrix}, \qquad \mathbf{Q}(\bar{t}) = f_x(\bar{t})\begin{pmatrix} \lambda \\ 1/\mu \end{pmatrix}, \qquad \mathbf{N}(\mathbf{x}) = \begin{pmatrix} x_1^{2n-1} \\ 0 \end{pmatrix} \tag{15}$$

The non-linear system (14) will be studied analytically (for periodic regimes) by means of a special transformation of the equations of motion, and the results will be tested numerically. Note that to obtain a correct analytical solution for the impact regimes one must keep the strongly non-linear term $\beta\mathbf{N}(\mathbf{x})$, starting from the first step of the analysis. In other words, no linear generating system for the impact regimes can be admitted.

3. ANALYTICAL STUDY

3.1. LINEAR MODAL ANALYSIS

The linear analysis is not the main purpose of the present work; however, as a preliminary step the linear natural frequencies of the model should be determined. These frequencies will be used for future treatment of non-linear results. The frequencies are given by considering the linear undamped system

$$\mathbf{B}\frac{\mathrm{d}^2\mathbf{x}}{\mathrm{d}\bar{t}^2} + \mathbf{K}\mathbf{x} = 0. \tag{16}$$

To determine the normal mode regime we assume the solution

$$\mathbf{x} = \mathbf{H}\cos\omega\bar{t}, \qquad \mathbf{H} = \begin{pmatrix} h_1 \\ h_2 \end{pmatrix}. \tag{17}$$

Substituting equation (17) into (16) gives a homogeneous set of algebraic equations for the amplitude,

$$(\mathbf{K} - \omega^2\mathbf{B})\mathbf{H} = 0, \tag{18}$$

and the frequency equation,

$$\det(\mathbf{K} - \omega^2\mathbf{B}) = 0 \Rightarrow \omega^4 - \frac{1+v^2}{1-\mu}\omega^2 + \frac{v^2}{1-\mu} = 0. \tag{19}$$

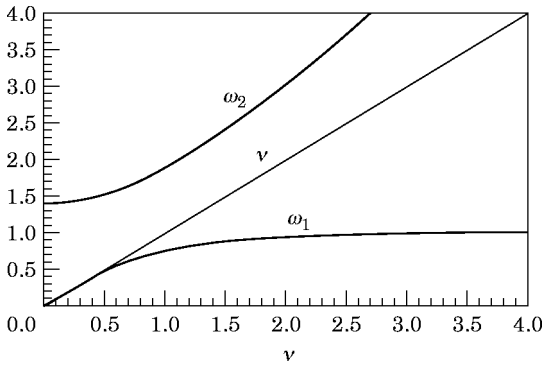

Figure 4. The dependence of the linear natural frequencies of the model on the partial frequency ratio $\nu = \omega_L/\omega_l$ for model parameters $\beta = 1$, $\lambda = 0{\cdot}5$ and $\mu = 0{\cdot}5$.

The roots of equation (19) are

$$\omega_1^2 = \frac{1 + \nu^2 + \sqrt{(1-\nu^2)^2 + 4\mu\nu^2}}{2(1-\mu)}, \qquad h_2 = \frac{\lambda\mu\omega_1^2}{\nu^2 - \omega_1^2} h_1, \qquad \text{in-phase mode,} \tag{20}$$

$$\omega_2^2 = \frac{1 + \nu^2 + \sqrt{(1-\nu^2)^2 + 4\mu\nu^2}}{2(1-\mu)}, \qquad h_2 = \frac{\lambda\mu\omega_2^2}{\nu^2 - \omega_2^2} h_1, \qquad \text{out-of-phase mode.} \tag{21}$$

The dependence of the linear modal frequencies on the local frequency ratio $\nu = \omega_L/\omega_l$ for fixed mass ratio parameter $\mu = 0{\cdot}5$ is illustrated in Figure 4. Careful inspection, together with Figure 4, shows that the following relationship holds:

$$\omega_1 < \nu < \omega_2. \tag{22}$$

This relationship will be used later.

It is known that the normal modes of any linear system are orthogonal with respect to the matrix **B**:

$$\mathbf{H}_1^{\mathrm{T}} \mathbf{B} \mathbf{H}_2 = 0, \tag{23}$$

where $\mathbf{H}_i$ is the eigenvector corresponding to the ith natural frequency ω_i.

3.2. NON-LINEAR PERIODIC REGIMES

Consider the free undamped oscillation of the non-linear system:

$$\mathbf{B} \frac{\mathrm{d}^2\mathbf{x}}{\mathrm{d}\bar{t}^2} + \mathbf{K}\mathbf{x} + \beta\mathbf{N}(\mathbf{x}) = 0. \tag{24}$$

If the non-linear terms appearing in the equations of motion are small compared with the linear terms, then the straight lines in the amplitudes plane $h_1 h_2$ predicted by linear theory, equations (20) and (21) will be slightly deformed.

To consider the strongly non-linear situation which results by including the power terms with a higher exponent, the STTT technique will be applied. The idea of STTT is similar to a great extent to the trigonometric generating functions $\{\sin\xi, \cos\xi\}$ frequently used in constructing solutions of linear and weakly non-linear systems. Similarly, one can consider a pair of non-smooth functions which have relatively simple forms and will be termed as the saw-tooth sine, $\tau(\xi)$, and the rectangular cosine, $e(\xi)$, which is the generalized derivative of $\tau(\xi)$, as shown in Figure 5. The functions $\{\tau(\xi), e(\xi)\}$ and $\{\sin\xi, \cos\xi\}$

describe the motions of the two simplest vibrating models; namely, the motion of a particle between two rigid barriers and a mass–spring oscillator, respectively.

We seek a family of periodic solutions of equations (24) in the form

$$\mathbf{x} = \mathbf{X}(\tau), \qquad \tau = \tau(\overline{t}/a), \tag{25}$$

where a is an unknown scaling factor which is equal to one-quarter of the period $T = 4a$ and must be defined for the autonomous case.

Thus the solution will be constructed as a function of the saw-tooth function τ, which varies in the region $-1 \leqslant \tau \leqslant 1$. Note that equation (24) admits a group of transformations $\mathbf{x} \to -\mathbf{x}$. As a result, the solution can be constructed as an odd function: $\mathbf{X}(-\tau) \equiv -\mathbf{X}(\tau)$.

When substituting equation (25) into equation (24), one should take into account the following differentiation scheme of the expression (25). Due to the equality $e^2(\overline{t}/a) = 1$, one can write

$$\frac{\mathrm{d}\mathbf{x}}{\mathrm{d}\overline{t}} = \frac{1}{a}\frac{\mathrm{d}\mathbf{X}}{\mathrm{d}\tau}e, \qquad \frac{\mathrm{d}^2\mathbf{x}}{\mathbf{d}\overline{t}^2} = \frac{1}{a^2}\frac{\mathrm{d}^2\mathbf{X}}{\mathrm{d}\tau^2} + \frac{1}{a^2}\frac{\mathrm{d}\mathbf{X}}{\mathrm{d}\tau}\frac{\mathrm{d}e(\overline{t}/a)}{\mathrm{d}(\overline{t}/a)}. \tag{26}$$

The last term in equation (26) contains the series of Dirac delta functions

$$\frac{\mathrm{d}e(\overline{t}/a)}{\mathrm{d}(\overline{t}/a)} = 2\sum_{j=-\infty}^{j=\infty}\left[\delta\left(\frac{\overline{t}}{a} + 1 - 4j\right) - \delta\left(\frac{\overline{t}}{a} - 1 - 4j\right)\right]. \tag{27}$$

Now that the delta functions (27) are "localized" at points $\{\overline{t}:\tau(\overline{t}/a) = \pm 1\}$. This means that under the condition

$$\mathrm{d}\mathbf{X}/\mathrm{d}\tau = 0 \qquad \text{for } \tau = \pm 1, \tag{28}$$

all delta functions of the series will be eliminated, and as a result the second derivative in equation (26) becomes a continuous function.

Substituting equation (26) into the equations of motion (24), one obtains the boundary

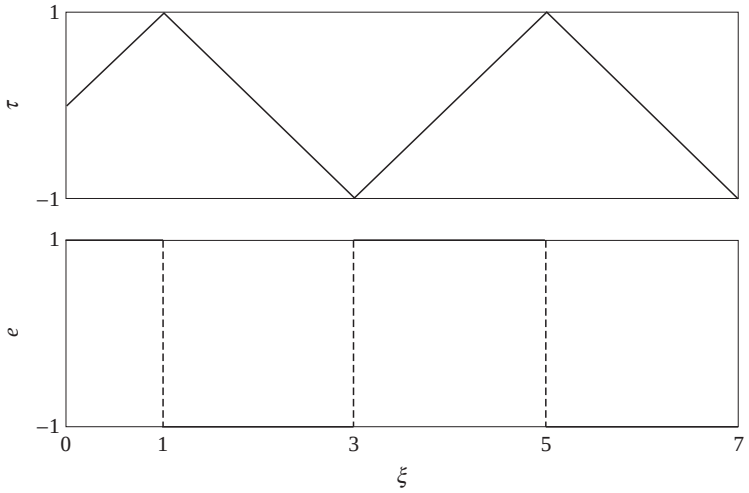

Figure 5. Saw-tooth sine and rectangular cosine.

value problem

$$\mathbf{B}\frac{\mathrm{d}^2\mathbf{X}}{\mathrm{d}\tau^2} = -a^2[\mathbf{K}\mathbf{X} + \beta\mathbf{N}(\mathbf{X})], \tag{29}$$

$$\left.\frac{\mathrm{d}\mathbf{X}}{\mathrm{d}\tau}\right|_{\tau=1} = 0, \qquad \mathbf{X}(-\tau) \equiv -\mathbf{X}(\tau). \tag{30}$$

Note that the left side of equation (29) does not include the linear stiffness term, and by setting the right side to zero, the left side does not represent a harmonic oscillator as in the case of quasi-linear treatment. This means that any generating solution for equation (29) should be based on the solution of $\mathbf{B}(\mathrm{d}^2\mathbf{X}/\mathrm{d}\tau^2) = 0$. However, by setting the right side to zero, the qualitative structure of the periodic motion of the system will be preserved. Note that this property will be destroyed if the same argument is applied to the system equations of motion before performing STTT. The transformed generating equation $\mathbf{B}(\mathrm{d}^2\mathbf{X}/\mathrm{d}\tau^2) = 0$ possesses a solution of the form $\mathbf{X}(\tau) = \mathbf{X}(0) + \mathbf{X}'(0)\tau$, which is a periodic function of $\overline{t}$. Now we seek a solution of the non-linear boundary value problem (29) and (30) in form of a series of successive approximations:

$$\mathbf{X} = \mathbf{X}_0(\tau) + \varepsilon\mathbf{X}_1(\tau) + \varepsilon^2\mathbf{X}_2(\tau) + \ldots, \qquad a^2 = \varepsilon h_0(1 + \varepsilon\gamma_1 + \varepsilon^2\gamma_2 + \ldots), \tag{31}$$

where the formal parameter $\varepsilon = 1$ is introduced as a book-keeping to identify terms of different orders in the expansion. Note that all terms of the first series are two-component column matrices: $\mathbf{X}_i(\tau) = (X_{i1}(\tau)\ \ X_{i2}(\tau))^{\mathrm{T}}$, $i = 0, 1, 2, \ldots$; these functions and the constants $h_0, \gamma_1, \gamma_2, \ldots$ will be defined by an iterative process.

Substituting equations (31) into equation (29) and considering terms of different orders of ε, one obtains the sequence of differential equations

$$\mathbf{B}\frac{\mathrm{d}^2\mathbf{X}_0}{\mathrm{d}\tau^2} = 0, \qquad \mathbf{B}\frac{\mathrm{d}^2\mathbf{X}_1}{\mathrm{d}\tau^2} = -h_0[\mathbf{K}\mathbf{X}_0 + \beta\mathbf{N}(\mathbf{X}_0)],$$

$$\mathbf{B}\frac{\mathrm{d}^2\mathbf{X}_2}{\mathrm{d}\tau^2} = -h_0\{\gamma_1[\mathbf{K}\mathbf{X}_0 + \beta\mathbf{N}(\mathbf{X}_0)] + [\mathbf{K} + \beta\mathbf{N}'_x(\mathbf{X}_0)]\mathbf{X}_1\}, \tag{32}$$

and so on, where $\mathbf{N}'_x(\mathbf{X})$ denotes the 2×2 matrix of the first partial derivatives of the column $\mathbf{N}(\mathbf{X})$ elements with respect to the components of vector $\mathbf{X}$. Higher order equations can also be generated; however, terms involved in the expression of $\mathbf{N}(\mathbf{X})$ are obtained using Taylor's expansion with respect to ε.

The boundary conditions (30) will be satisfied starting from the second step of the iterative process; i.e., the sequence of boundary conditions for equations (32) is taking the form ($\varepsilon = 1$)

$$\left(\frac{\mathrm{d}\mathbf{X}_0}{\mathrm{d}\tau} + \frac{\mathrm{d}\mathbf{X}_1}{\mathrm{d}\tau}\right)\Bigg|_{\tau=1} = 0, \qquad \left.\frac{\mathrm{d}\mathbf{X}_2}{\mathrm{d}\tau}\right|_{\tau=1} = 0, \ldots. \tag{33}$$

The first equality in equation (33) implies that the derivatives $\mathrm{d}\mathbf{X}_0/\mathrm{d}\tau$ and $\mathrm{d}\mathbf{X}_1/\mathrm{d}\tau$ at the point $\tau = 1$ are assumed to be of the same order, although the functions $\mathbf{X}_0$ and $\mathbf{X}_1$ are of differing orders of magnitude, as the series (31) indicates. Note that if each of the derivatives $\mathrm{d}\mathbf{X}_0/\mathrm{d}\tau$ and $\mathrm{d}\mathbf{X}_1/\mathrm{d}\tau$ is separately set to zero at the point $\tau = 1$, then one can only obtain the trivial solution $\mathbf{X} \equiv \mathbf{0}$.

Having no boundary conditions at the first step of the process, one obtains the following

generating solution:

$$\mathbf{X}_0 = \mathbf{A}_0\tau, \qquad \mathbf{A}_0 = (A_{01} \quad A_{02})^{\mathrm{T}} = \text{constant}. \tag{34}$$

This solution describes a vibro-impact oscillator with two rigid barriers where the length of the arbitrary vector $\mathbf{A}_0$ is equal to the barrier spacing. The direction of the vector will be defined in the next approximation.

Substituting equation (34) into the second differential equation of the sequence (32) and integrating with respect to τ gives

$$\mathbf{X}_1 = \mathbf{A}_1\tau + \mathbf{K}_{1,3}\tau^3 + \mathbf{K}_{1,2n+1}\tau^{2n+1}, \tag{35}$$

where $\mathbf{A}_1$ is an arbitrary constant vector:

$$\mathbf{K}_{1,3} = -\frac{h_0}{6}\mathbf{B}^{-1}\mathbf{K}\mathbf{A}_0, \qquad \mathbf{K}_{1,2n+1} = -\frac{h_0\beta}{2n(2n+1)}\mathbf{B}^{-1}\mathbf{N}(\mathbf{A}_0).$$

The inverse matrix $\mathbf{B}^{-1}$ exists if the following condition holds:

$$\det \mathbf{B} = 1/(\lambda\mu) - 1 \neq 0.$$

In terms of the original system parameters, this condition implies that $ml \neq ML$. Note that the first term in equation (35) has the same structure as the generating solution (34), and thus, there is no need to keep this term in equation (35). Accordingly, one should set $\mathbf{A}_1 = 0$. Combining two members of the expansion, $\mathbf{X}_0$ and $\mathbf{X}_1$, and satisfying the first boundary condition in equation (33), one obtains the non-linear eigenvector problem relating to the vector $\mathbf{A}_0$:

$$\left(\mathbf{K} - \frac{2}{h_0}\mathbf{B}\right)\mathbf{A}_0 + \frac{\beta}{n}\mathbf{N}(\mathbf{A}_0) = 0. \tag{36}$$

When the impact parameter $\beta = 0$, the problem (36) is reduced to a linear eigenvector problem of the type (18), and a comparison with equation (19) shows that the value $2/h_0$ coincides with the square of the linear normal mode natural frequency (ω_1^2 or ω_2^2). In the linear case the natural frequencies do not depend on the eigenvector $\mathbf{A}_0$. If the non-linearity exists, a relationship between the frequency and the amplitude vector is established by multiplying equation (36) by the transpose of the vector $\mathbf{A}_0$. This relationship is given by the expression

$$\frac{2}{h_0} = \frac{\mathbf{A}_0^{\mathrm{T}}\mathbf{K}\mathbf{A}_0}{\mathbf{A}_0^{\mathrm{T}}\mathbf{B}\mathbf{A}_0} + \frac{\beta}{n}\frac{\mathbf{A}_0^{\mathrm{T}}\mathbf{N}(\mathbf{A}_0)}{\mathbf{A}_0^{\mathrm{T}}\mathbf{B}\mathbf{A}_0}. \tag{37}$$

Problem (36) will be considered later.

Now let us consider the next step of the iteration process. Substituting equations (34) and (35) into the third equation of equation (32) and integrating gives

$$\mathbf{X}_2 = \mathbf{A}_2\tau + \gamma_1\mathbf{X}_1 + \mathbf{K}_{2,5}\tau^5 + \mathbf{K}_{2,2n+3}\tau^{2n+3} + \mathbf{K}_{2,4n+1}\tau^{4n+1}, \tag{38}$$

where $\mathbf{A}_2$ is an arbitrary constant vector, and

$$\mathbf{K}_{2,5} = -\frac{h_0}{20}\,\mathbf{B}^{-1}\mathbf{K}\mathbf{K}_{1,3},$$

$$\mathbf{K}_{2,2n+3} = -\frac{h_0}{(2n+2)(2n+3)}\,\mathbf{B}^{-1}[\beta\mathbf{N}'_x(\mathbf{A}_0)\mathbf{K}_{1,3} + \mathbf{K}\mathbf{K}_{1,2n+1}],$$

$$\mathbf{K}_{2,4n+1} = -\frac{\beta h_0}{4n(4n+1)}\,\mathbf{B}^{-1}\mathbf{N}'_x(\mathbf{A}_0).$$

Solution (38) contains an arbitrary vector $\mathbf{A}_2$ and an arbitrary scalar γ_1. The arbitrary vector $\mathbf{A}_2$ cannot be set to zero as in the case of the $\mathbf{X}_1$ solution, because the boundary condition (33) will result in two equations for one unknown γ_1. In this case one has to determine $\mathbf{A}_2$ and γ_1. First, the boundary condition (33) for $\mathbf{X}_2$ gives

$$\mathbf{A}_2 = \gamma_1\mathbf{A}_0 - 5\mathbf{K}_{2,5} - (2n+3)\mathbf{K}_{2,2n+3} - (4n+1)\mathbf{K}_{2,4n+1}. \tag{39}$$

However, this matrix equation contains three unknowns in two equations, and one should adopt another condition to determine these unknowns. The initial velocity vector $\dot{\mathbf{x}}(0)$ should preserve its projection on $\mathbf{A}_0$ with respect to the inertia matrix $\mathbf{B}$ on each of steps of the iterative process; i.e.,

$$\mathbf{A}_0^{\mathrm{T}}\mathbf{B}\dot{\mathbf{x}}(0) = \frac{1}{a}\,\mathbf{A}_0^{\mathrm{T}}\mathbf{B}(\mathbf{A}_0 + \mathbf{A}_1 + \mathbf{A}_2) = \frac{1}{a}\,\mathbf{A}_0^{\mathrm{T}}\mathbf{B}\mathbf{A}_0.$$

This leads to the condition of the $\mathbf{B}$-orthogonality of the vector $\mathbf{A}_2$ with respect to $\mathbf{A}_0$; i.e.,

$$\mathbf{A}_0^{\mathrm{T}}\mathbf{B}\mathbf{A}_2 = 0. \tag{40}$$

The geometrical meaning of condition (40) is that a component of the solution, which is proportional to the saw-tooth time mode τ, preserves its $\mathbf{B}$-orthogonal projection on the generating solution $\mathbf{A}_0\tau$ on the second step of the iteration process. Basically, this is a normalization condition.

Substituting equation (39) into equation (40) the parameter γ_1 is determined by the expression

$$\gamma_1 = 5\,\frac{\mathbf{A}_0^{\mathrm{T}}\mathbf{B}\mathbf{K}_{2,5}}{\mathbf{A}_0^{\mathrm{T}}\mathbf{B}\mathbf{A}_0} + (2n+3)\,\frac{\mathbf{A}_0^{\mathrm{T}}\mathbf{B}\mathbf{K}_{2,2n+3}}{\mathbf{A}_0^{\mathrm{T}}\mathbf{B}\mathbf{A}_0} + (4n+1)\,\frac{\mathbf{A}_0^{\mathrm{T}}\mathbf{B}\mathbf{K}_{2,4n+1}}{\mathbf{A}_0^{\mathrm{T}}\mathbf{B}\mathbf{A}_0}. \tag{41}$$

Thus, the second approximation is completed. Similar calculations can be performed to compute higher order approximations.

To illustrate the solution structure in more detail, the approximate solution in terms of its component is written

$$x_1 = A_{01}\tau - \frac{h_0(\lambda A_{01} - v^2 A_{02})}{\lambda(1-\mu)}\,\frac{\tau^3}{6} - \frac{\beta h_0 A_{01}^{2n-1}}{\lambda(1-\mu)}\,\frac{\tau^{2n+1}}{2n(2n+1)} + \ldots, \tag{42}$$

$$x_2 = A_{02}\tau + \frac{h_0(\lambda\mu A_{01} - v^2 A_{02})}{(1-\mu)}\,\frac{\tau^3}{6} + \frac{\mu\beta h_0 A_{01}^{2n-1}}{(1-\mu)}\,\frac{\tau^{2n+1}}{2n(2n+1)} + \ldots, \tag{43}$$

where $\tau = \tau(\bar{t}/a)$, $a^2 = h_0(1 + \gamma_1 + \ldots)$, and

$$\gamma_1 = \left[-\frac{\beta^2 h_0^2 (1-2n) A_{01}^{4n-2}}{8\lambda(1-\mu)n^2(1+2n)} + \frac{\beta h_0^2 (3-4n+4n^2)(\lambda A_{01} - v^2 A_{02}) A_{01}^{2n-1}}{12\lambda(1-\mu)n(1+2n)} \right.$$

$$\left. + \frac{h_0^2(\lambda^2 \mu A_{01}^2 - 2\lambda\mu v^2 A_{01} A_{02} + v^4 A_{02}^2)}{24\lambda(1-\mu)\mu} \right] \Bigg/ \left(2A_{01}A_{02} + \lambda A_{01}^2 + \frac{A_{02}^2}{\lambda\mu} \right). \tag{44}$$

To complete the solution, one must obtain the components of the vector $\mathbf{A}_0 = (A_{01} \;\; A_{02})^{\mathrm{T}}$ by solving the non-linear eigenvector problem (36) (the solution is given in the next subsection). In the linear case ($\beta = 0$) the vector amplitude remains indefinite, although its direction is preserved. If the non-linearity exists ($\beta \neq 0$) then, as follows from equation (37), the vector length depends on the parameter h_0. Thus, the solution given by equations (42)–(44) includes one constant parameter h_0. Since the equation of motion (24) admits a group of time shift $\bar{t} \to \bar{t} + \alpha$, another arbitrary parameter α can always be introduced into the solution. Finally, the solution will contain two parameters h_0 (or the length of eigenvector can be chosen), and phase α. Using these parameters, one can satisfy a definite type of initial conditions which provide the existence of the periodic regimes.

3.3. THE NON-LINEAR EIGENVECTOR PROBLEM

Consider the non-linear eigenvalue problem (36), which can be written in terms of the vector components using the notations (15):

$$\lambda(1 - \Omega_0^2)A_{01} - \Omega_0^2 A_{02} + \frac{\beta}{n} A_{01}^{2n-1} = 0, \tag{45}$$

$$\Omega_0^2 A_{01} - \frac{1}{\lambda\mu}(v^2 - \Omega_0^2)A_{02} = 0, \tag{46}$$

where $\Omega_0^2 = 2/h_0$.

Equation (46) gives

$$A_{02} = \lambda\mu \frac{\Omega_0^2}{v^2 - \Omega_0^2} A_{01}. \tag{47}$$

Substituting equation (47) into equation (45) and using equations (19)–(21), one obtains

$$\beta A_{01}^{2n-2} = n\lambda(1-\mu) \frac{(\Omega_0^2 - \omega_1^2)(\Omega_0^2 - \omega_2^2)}{\Omega_0^2 - v^2}. \tag{48}$$

If $\beta = 0$ one has the linear case, and equation (48) should be considered as an equation for linear frequencies with respect to Ω_0. In the non-linear case ($\beta \neq 0$) equation (48) defines an amplitude A_{01} as a function of Ω_0. Having this function, one can find another amplitude A_{02} by means of the expression (47). Assuming that the mass ratio parameter μ to be less than 1, and taking into account equation (22), i.e., $\omega_1 < v < \omega_2$, one obtains the following condition for equation (48):

$$\omega_1 < \Omega_0 < v \qquad \text{or} \qquad \omega_2 < \Omega_0. \tag{49}$$

Taking Ω_0 as a variable parameter, one can say that expressions (47) and (48) define two curves on the plane $A_{01}A_{02}$ (indicated by solid curves in Figures 6(a, b):

$$A_{01} = A_{01}(\Omega_0), \quad A_{02} = A_{02}(\Omega_0) \qquad (\omega_1 < \Omega_0 < v); \tag{50}$$

$$A_{01} = A_{01}(\Omega_0), \quad A_{02} = A_{02}(\Omega_0) \qquad (\omega_2 < \Omega_0). \tag{51}$$

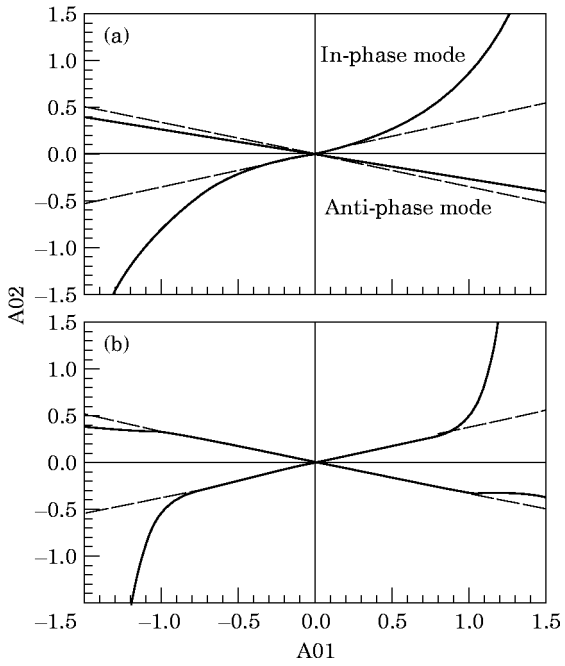

Figure 6. Linear and non-linear eigenvectors for system parameters $\beta = 1$, $\lambda = 0{\cdot}5$, $\mu = 0{\cdot}5$, $\nu = 1$. (a) $n = 2$; (b) $n = 6$. — —, Linear normal modes; ——, non-linear normal modes.

Each point of these curves represents approximate values of amplitudes for strongly non-linear out-of-phase (50) and in-phase (51) periodic regimes. If the parameter Ω_0 is close to one of the linear natural frequencies ω_1 or ω_2, then the curves (50) or (51) go close to a straight line of one of the linear normal modes (20) or (21). Figure 6(a) is obtained for the case $n = 2$, while Figure 6(b) is for $n = 6$. For a given point (A_{01}, A_{02}) belonging to one curve the amplitudes of the pendulum and the tank $(\hat{x}_1, \hat{x}_2)$ can be obtained by using expressions (42) and (43), for $\tau = 1$. The estimated amplitudes for the out-of-phase and in-phase motions are shown in Figure 7. For the out-of-phase mode the relationship is represented by an almost straight line for both small and large amplitudes. In the case of a strongly non-linear regime, when the pendulum amplitude is $\hat{x}_1 \approx 1$, the tank amplitude

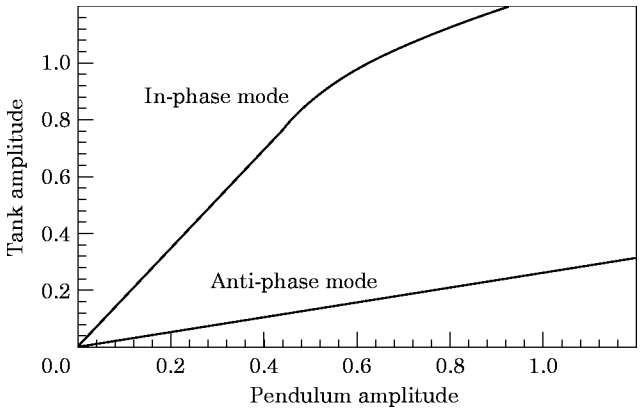

Figure 7. The tank and pendulum amplitude relationships of non-linear in-phase and anti-phase periodic free oscillation regimes, for model parameters $n = 6$, $\beta = 1$, $\lambda = 0{\cdot}5$, $\mu = 0{\cdot}5$ and $\nu = 0{\cdot}5$.

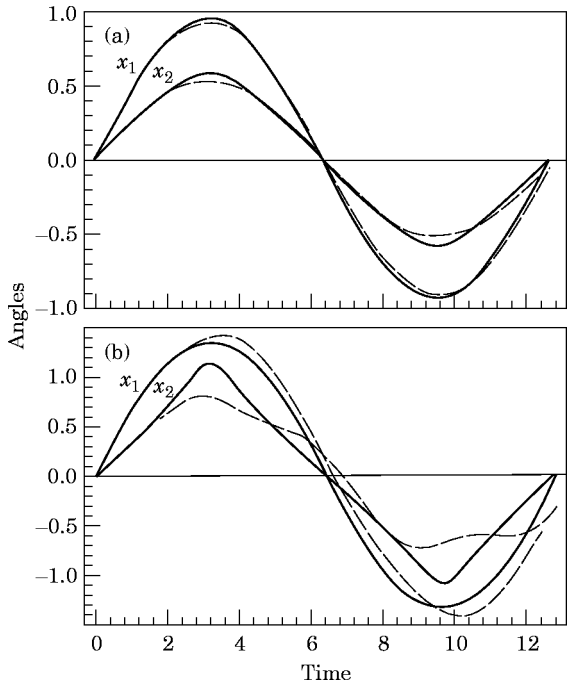

Figure 8. One period time history records of in-phase mode for model parameters $n = 6$, $\beta = 1$, $\lambda = 0{\cdot}5$, $\mu = 0{\cdot}5$ and $\nu = 0{\cdot}5$. — —, Numerical solution; ——, analytical solution. (a) $\Omega_0^2 - \omega_1^2 = 0{\cdot}001$; (b) $\Omega_0^2 - \omega_1^2 = 0{\cdot}005$.

is relatively small, at $\hat{x}_2 \approx 0{\cdot}2$. Another situation is observed for the in-phase mode, when both the pendulum and the tank simultaneously move in the same direction. The tank amplitude is large enough compared to the pendulum, and the curve slope is not constant in the non-linear region (Figure 7, top curve). Numerical simulations also show that due to impact non-linearity the in-phase periodic regime is not stable with respect to small perturbations of the out-of-phase mode, and as a result the analytical and numerical solutions for the strongly non-linear in-phase regime (Figure 8(b)) are not as good as for the out-of-phase one (Figures 9(a) and (b)). In Figures 8(a) and 8(b) is shown a comparison between the numerical estimation (shown by dashed curves) and the analytical result (shown by solid curves in the time domain for two values of the nearness of the non-linear natural frequency to the linear natural frequency; i.e., for $\Omega_0^2 - \omega_1^2 = 0{\cdot}001$ and $0{\cdot}005$ and for $n = 6$). Figure 8 is taken for the in-phase mode and shows that, for a large difference between the non-linear natural frequency and the linear one, the matching between numerical and analytical solutions is relatively poor. On the other hand, Figure 9 is obtained for the out-of-phase mode and reveals good agreement between the numerical and analytical solutions.

3.4. PARAMETRIC EXCITATION

Consider equation (14), under purely parametric excitation $\mathbf{P}(\bar{t})$ of period $T = 2a$. This means that the external force contains only a vertical periodic component $f_y(\bar{t})$ of the period $T = 2a$, and $\mathbf{Q}(\bar{t}) \equiv 0$. Therefore, we assume that the excitation period is equal to one half of the period of solution. Suppose that a time symmetry of function $f_y(\bar{t})$ allows us to introduce a new argument τ as $f_y(\bar{t}) \equiv f_y(a\tau(\bar{t}/a))$. For example, it can be verified that

$$f_y(\bar{t}) = p_0 \cos(\pi\bar{t}/a) \equiv p_0 \cos \pi\tau. \tag{52}$$

Taking this remark into account, one finally obtains, instead of equation (29), the transformed equation

$$\mathbf{B}\frac{\mathrm{d}^2\mathbf{X}}{\mathrm{d}\tau^2} = -a^2[\mathbf{K}\mathbf{X} + \mathbf{P}(\tau)\mathbf{X} + \beta\mathbf{N}(\mathbf{X})] \tag{53}$$

and the boundary conditions

$$\left.\frac{\mathrm{d}\mathbf{X}}{\mathrm{d}\tau}\right|_{\tau=1} = 0, \qquad \mathbf{X}(-\tau) \equiv -\mathbf{X}(\tau), \tag{54}$$

where

$$\mathbf{P}(\tau) = f_y(a\tau(\bar{t}/a))\begin{pmatrix} -\lambda & 0 \\ 0 & 1/\mu \end{pmatrix}.$$

To solve the boundary value problem (53) and (54), one can apply the iterative process presented in section 3.2. The only difference is that the left side part of the expansion (31) for a^2 is known, and one should additionally consider the parametric excitation term $\mathbf{P}(\tau)\mathbf{X}$.

For example, the expression (35) will take the form

$$\mathbf{X}_1 = \mathbf{K}_{1,3}\tau^3 + \mathbf{K}_{1,2n+1}\tau^{2n+1} - h_0\int_0^\tau (\tau - z)\mathbf{B}^{-1}\mathbf{P}(z)\mathbf{A}_0 z\,\mathrm{d}z. \tag{55}$$

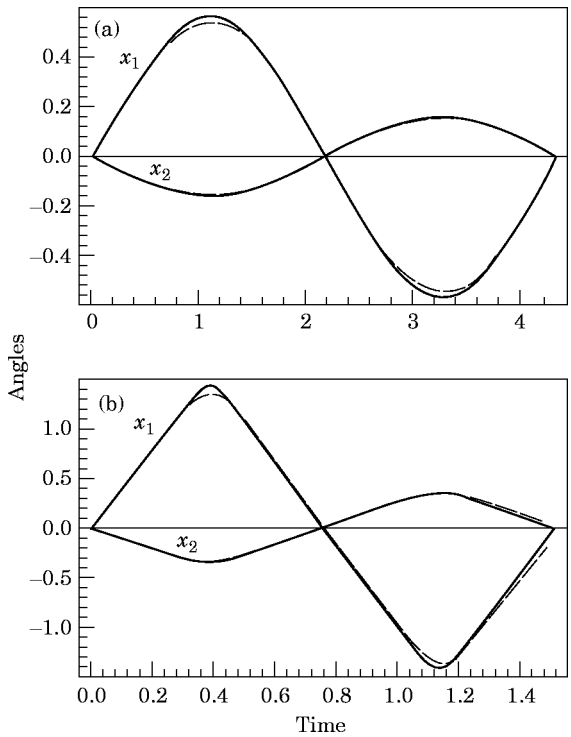

Figure 9. One period time history records of anti-phase mode for model parameters $n = 6$, $\beta = 1$, $\lambda = 0{\cdot}5$, $\mu = 0{\cdot}5$ and $\nu = 0{\cdot}5$. — —, Numerical solution; ——, analytical solution. (a) $\Omega_0^2 - \omega_2^2 = 0{\cdot}02$; (b) $\Omega_0^2 - \omega_2^2 = 30$.

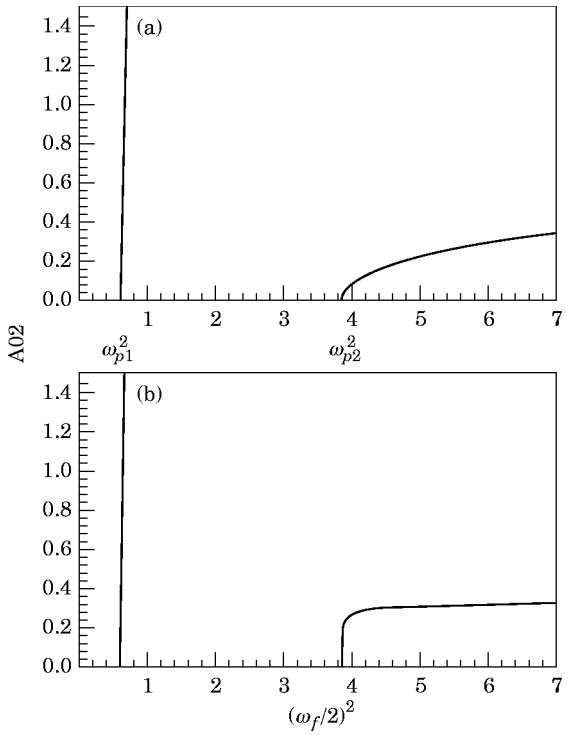

Figure 10. Parametric resonance curves for in-phase and anti-phase modes for model parameters $\beta = 1$, $\lambda = 1$, $\mu = 0{\cdot}5$, $v = 0{\cdot}5$, $p_0 = 1{\cdot}07$. (a) $n = 2$; (b) $n = 6$.

Recall that, in the present formulation, we seek an odd solution with respect to τ, so that the integral term in equation (63) must be odd. This will lead to a restriction for the parametric force considered; namely, the function $\mathbf{P}(\tau)$ must be even. Note that this restriction can be relaxed in a more general formulation.

The non-linear eigenvector problem relating the vector $\mathbf{A}_0$ is written as

$$\left(\mathbf{K} + 2\int_0^1 \mathbf{P}(z)z\,\mathrm{d}z - \Omega_0^2\mathbf{B}\right)\mathbf{A}_0 + \frac{\beta}{n}\,\mathbf{N}(\mathbf{A}_0) = 0, \tag{56}$$

where $\Omega_0^2 = 2/h_0$.

Consider the non-linear eigenvector problem (56), which can be written in terms of its components as

$$\lambda(1 - \Omega_0^2 - p)A_{01} - \Omega_0^2 A_{02} + \frac{\beta}{n}\,A_{01}^{2n-1} = 0, \tag{57}$$

$$\Omega_0^2 A_{01} - \frac{1}{\lambda\mu}\,(v^2 - \Omega_0^2 + \lambda p)A_{02} = 0, \tag{58}$$

where $p = 2\int_0^1 f_y(az)z\,\mathrm{d}z$.

Equation (58) gives

$$A_{02} = \lambda\mu\,\frac{\Omega_0^2}{v^2 - \Omega_0^2 + \lambda p}\,A_{01}. \tag{59}$$

Substituting equation (59) into equation (57), one obtains

$$\beta A_{01}^{2n-2} = n\lambda(1-\mu)\frac{(\Omega_0^2-\omega_{p1}^2)(\Omega_0^2-\omega_{p2}^2)}{\Omega_0^2-\nu^2-\lambda p}, \tag{60}$$

where ω_{p1} and ω_{p2} are the linear resonance frequencies of the system defined by the two roots

$$\omega_{p1,2}^2 = \frac{\omega_1^2+\omega_2^2}{2} - \frac{p}{2}\frac{1-\lambda}{1-\mu} \pm \left[\left(\frac{\omega_1^2-\omega_2^2}{2}\right)^2 - p\frac{1-\lambda}{1-\mu}\left(\frac{\omega_1^2+\omega_2^2}{2} - \frac{\nu^2-\lambda}{1-\lambda}\right) + \frac{p^2}{4}\frac{(1+\lambda)^2-4\lambda\mu}{(1-\mu)^2}\right]^{1/2}.$$

The parametric excitation linear resonance frequencies are $2\omega_{p1}$ and $2\omega_{p2}$. The dependence of the vector component A_{02} on the external parametric excitation frequency is shown in Figure 10. The excitation has been expressed by relation (52). For this case, we have $p = -4p_0/\pi^2$. Note that the vector component A_{02} gives estimate for the tank amplitude and can be used for qualitative consideration, although more accurate results can be obtained in a manner similar to the previous subsection.

In Figures 11(a) and 11(b) are shown time history records of the pendulum and tank motions obtained by numerical integration of equation (53) for a parametric resonance condition corresponding to the first and second modes, respectively. Initially, the system is almost at rest (very small initial conditions are used: $x_1(0) = x_2(0) = 0$; $\dot{x}_1(0) = 0{\cdot}01$, (a)$\dot{x}_2(0) = 0{\cdot}007$, (b) $\dot{x}_2(0) = -0{\cdot}003$). If the excitation frequency ω_f is close to $2\omega_{p1}$ or to $2\omega_{p2}$, then oscillations of large amplitudes appear. Asymmetry of the curves indicates that the low frequency oscillations involve both in-phase and out-of-phase motions (Figure 11(a)). On the other hand, the out-of-phase mode is mainly excited about the higher frequency (Figure 11(b)). This conclusion is confirmed by the configuration plane representation for trajectories of the solutions shown in Figures 11(c) and (d). The upper two configuration planes (Figure 11(c)) are obtained for two trajectory periods, $t^{max} = 16{\cdot}5$ and 66, when the first mode is parametrically excited, while the lower graphs (Figure 11(d)) are obtained when the second mode is parametrically excited. In both cases, it is seen that in-phase motion is always transformed to out-of-phase motion.

3.5. LATERAL PERIODIC LOADING

Consider equation (14) with $\mathbf{P}(\bar{t}) \equiv 0$, and let $\mathbf{Q}(\bar{t})$ to be a periodic function with period $T = 4a$. This means that the external force contains only horizontal periodic component $f_x(\bar{t})$ of period $T = 4a$. Suppose that a time symmetry of the function $f_x(\bar{t})$ allows one to introduce a new argument τ as $f_x(\bar{t}) \equiv f_x(a\tau(\bar{t}/a))$. Note that the technique considered does not require any harmonic analysis of external forces, such as Fourier expansions. Instead, periodic functions can be approximated by power series with respect to the saw-tooth 'sine τ'. The first approximation step is expressed by the linear function with respect to τ term (see, for example, the solutions constructed). To illustrate operations with the saw-tooth approximation for an external force, consider the example

$$f_x(\bar{t}) = p_0\tau(\bar{t}/a). \tag{61}$$

It follows from the transformations below that the solution can be easily rewritten for another kind of external force, which in the present formulation must be an odd function

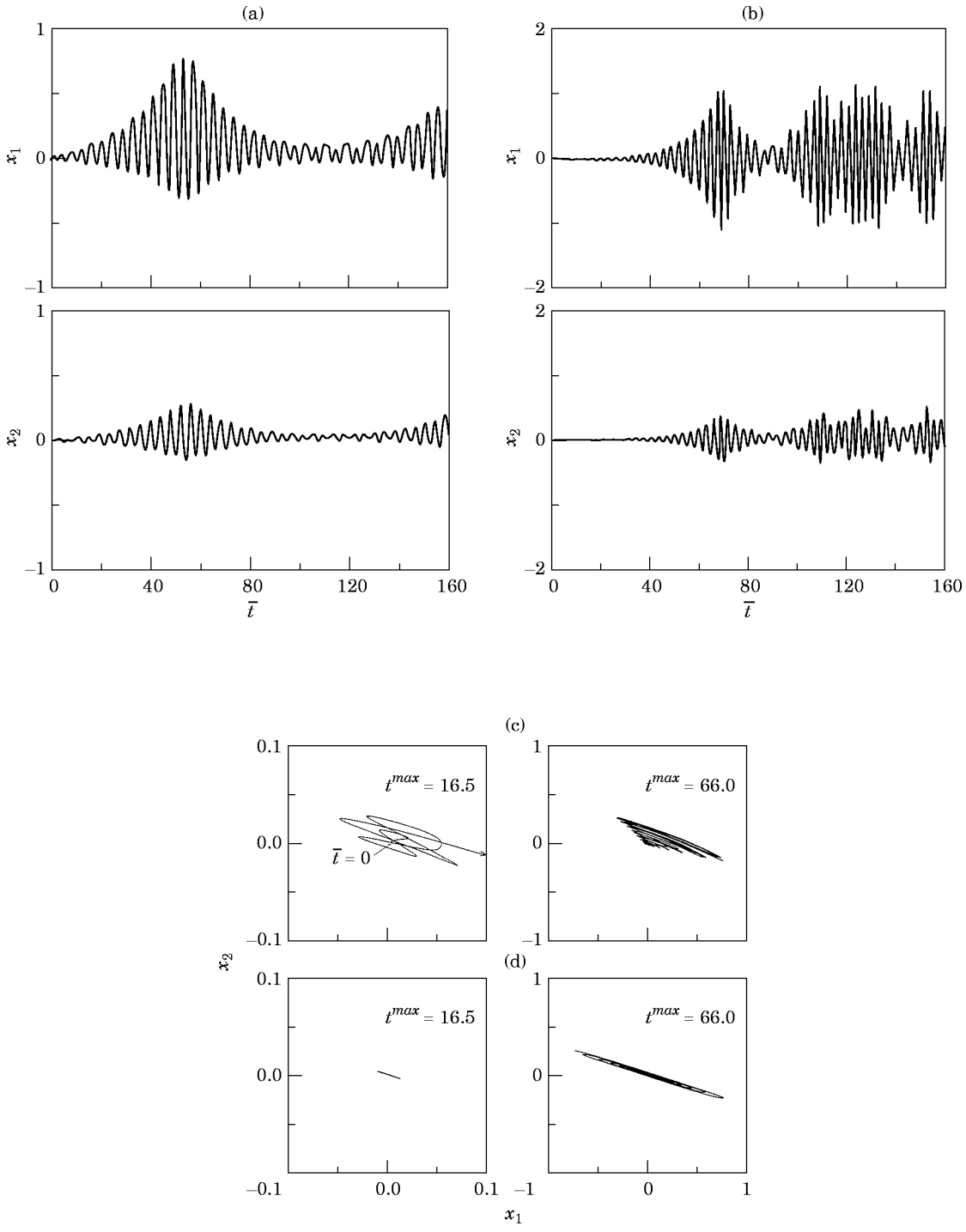

Figure 11. Time history response records under parametric excitation of (a) the first mode, i.e., $\omega_f = \omega_{p1}/2$, for model parameters $n = 6$, $\beta = 1$, $\lambda = 0{\cdot}5$, $\mu = 0{\cdot}5$, $\nu = 1$, $d_1 = 0{\cdot}01$, $d_2 = 0{\cdot}01$ and $p_0 = 1{\cdot}07$; (*b*) the second mode, i.e., $\omega_f = \omega_{p2}/2$; and trajectories of the modal amplitudes in the configuration plane for (c) $\omega_f = \omega_{p1}/2$ and (d) $\omega_f = \omega_{p2}/2$.

of τ. Taking this remark into account, one finally obtains, instead of equation (29), the transformed equation

$$\mathbf{B}\frac{\mathrm{d}^2\mathbf{X}}{\mathrm{d}\tau^2} = -a^2[\mathbf{K}\mathbf{X} + \beta\mathbf{N}(\mathbf{X}) - \mathbf{Q}(\tau)], \tag{62}$$

where $\mathbf{Q}(\tau) = p_0\tau(-\lambda, 1/\mu)^{\mathrm{T}}$ and the boundary conditions are the same as equations (54).

For this case the first step of the iteration process gives

$$\mathbf{X}^1 = \mathbf{K}_3^1\tau^3 + \mathbf{K}_{2n+1}^1\tau^{2n+1} - h_0\int_0^\tau (\tau - z)\mathbf{B}^{-1}\mathbf{Q}(z)\,\mathrm{d}z. \tag{63}$$

The boundary conditions lead to the following matrix equation with respect to the constant vector $\mathbf{A}_0$:

$$(\mathbf{K} - \Omega_0^2\mathbf{B})\mathbf{A}_0 + \frac{\beta}{n}\mathbf{N}(\mathbf{A}_0) = 2\int_0^1 \mathbf{Q}(z)\,\mathrm{d}z. \tag{64}$$

For the example considered, one finally obtains

$$A_{02} = \lambda\mu\frac{\Omega_0^2}{\nu^2 - \Omega_0^2}A_{01} + \frac{\lambda p_0}{\nu^2 - \Omega_0^2}, \tag{65}$$

$$\beta A_{01}^{2n-1} = n\lambda(1-\mu)\frac{(\Omega_0^2 - \omega_1^2)(\Omega_0^2 - \omega_2^2)}{\Omega_0^2 - \nu^2}A_{01} - \frac{n\lambda\nu^2}{\Omega_0^2 - \nu^2}p_0. \tag{66}$$

These two expressions are used in constructing the frequency–amplitude curves of the pendulum A_{01} shown in Figures 12(a) and 12(b), where $2/h_0 = \Omega_0^2(A_{01})$, for a fixed parameter of the force amplitude p_0 and two different exponent of the non-linearity $n = 2$, and 6, respectively. For the small amplitude region, the curves behave like a typical linear oscillator with linear natural frequencies. In the non-linear region, i.e., for sufficiently large A_{01}, the curves essentially depend on the impact power non-linearity n. It is observed that a large exponent $n = 6$ results in an almost vertical portion of the out-of-phase mode curve in the region of higher excitation frequency $\Omega_0 > \omega_2$. This means that the pendulum amplitude in the out-of-phase periodic regime becomes almost fixed, when the excitation frequency Ω_0 satisfies the condition $\Omega_0 > \omega_2$.

4. CONCLUSIONS

The non-linear interaction of liquid free surface impact motion, the support structure dynamics has been considered. The impact is modelled based on a phenomenological representation in the form of a power function with a higher exponent. A special saw-tooth time transformation (STTT) technique has been applied to analyze the strongly non-linear periodic regimes of the in-phase and out-of-phase modes. Based on explicit forms of analytical solutions, all basic non-linear free and forced response characteristics in terms of time and frequency domains are obtained. The results have shown that a high frequency out-of-phase non-linear mode appears with a relatively small tank amplitude and preserves stability with respect to small perturbations of the in-phase oscillation mode. The in-phase mode is excited by a low frequency forcing function and then may be realized first during a transient period when the model starts its motion.

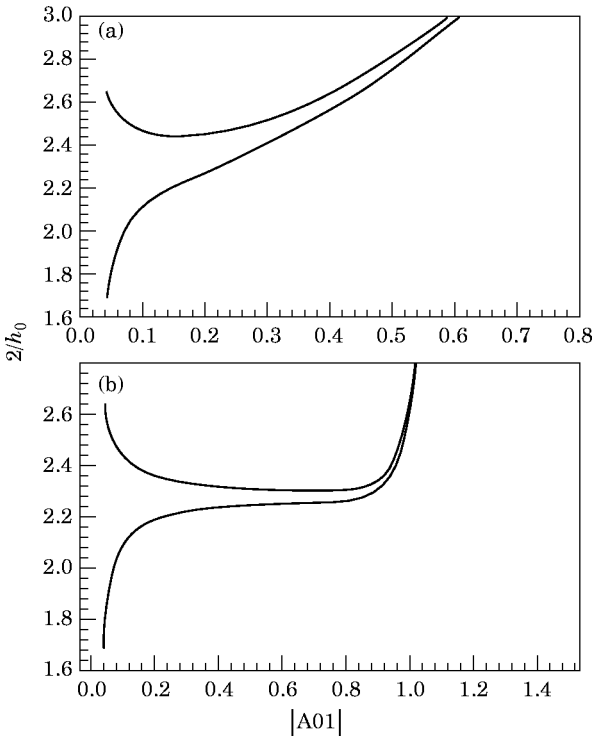

Figure 12. Amplitude–frequency resonance curves under lateral periodic excitation for two powers of non-linearity: (a) $n = 2$, (b) $n = 6$. Model parameters $\beta = 1$, $\lambda = 0{\cdot}5$, $\mu = 0{\cdot}5$, $\nu = 0{\cdot}5$, and $p_0 = 0{\cdot}07$.

ACKNOWLEDGMENTS

This research is supported by National Science Foundation grant No. CMS-9634223, and by the Institute for Manufacturing Research at Wayne State University.

REFERENCES

1. H. N. Abramson (editor) 1966 *The Dynamic Behavior of Liquids in Moving Containers*. NASA SP 106.
2. D. A. Gustafson and G. R. Gustafson 1969 *Heavy Vehicle Overturning Problems* (in Swedish). Gothenburg, Sweden: Chalmer's Institute of Technology.
3. H. Isermann 1970 *Die Kippgrenze von Sattelkraftfahrzeugen mit fester und flussiger Ladung*. Deutsche Kraftfahrtforschung und Strassenverkehrstechnik, Heft 200.
4. H. F. Bauer 1972 *Vehicle System Dynamics* **1**, 227–260. On the destabilizing effect of liquids in various vehicles.
5. A. Slibar and H. Troger 1975 in *Proceedings of IUTAM Symposium*, 1975-08-18-22. Dynamic steady state behavior of a tractor–semitrailer-system carrying liquid load.
6. A. Slibar and H. Troger 1977 in *VSD–IUTAM Symposium*. The steady state behavior of tank trailer roads and trucks.
7. L. Strandberg 1978 *Lateral Stability of Road Tankers*. VTI Rapport, Nr. 138A, Sweden.
8. R. A. Ibrahim and A. D. S. Barr 1975 *Journal of Sound and Vibration* **42**, 159–179. Autoparametric resonance in a structure containing liquid, part I: two mode interaction.
9. R. A. Ibrahim and A. D. S. Barr 1975 *Journal of Sound and Vibration* **42**, 181–200. Autoparametric resonance in a structure containing a liquid, part II: three-mode interaction.
10. R. A. Ibrahim 1976 *Journal of Engineering for Industry* **98**, 1092–1098. Multiple internal resonance in a structure–liquid system.

11. R. A. Ibrahim, J.-S. Gau and A. Soundararajan 1988 *Journal of Sound and Vibration* **121**, 413–428. Parametric and autoparametric vibrations of an elevated water tower, part I: parametric response.
12. R. A. Ibrahim and W. Li 1988 *Journal of Sound and Vibration* **121**, 429–444. Parametric and autoparametric vibrations of an elevated water tower part II: autoparametric response.
13. A. Soundararajan and R. A. Ibrahim 1988 *Journal of Sound and Vibration* **121**, 445–462. Parametric and autoparametric vibrations of an elevated water tower, part III: random response.
14. P. A. Cox, E. B. Bowels and R. L. Bass 1980 *Evaluation of Liquid Dynamic Loads in Slack LNG Cargo Tanks*, Southwest Research Institute, San Antonio, Technical Report SR-1251.
15. W. Goldsmith 1960 *Impact*. London: Edward Arnold.
16. W. Johnson 1972 *Impact Strength of Materials*. London: Edward Arnold.
17. A. E. Kobrinsky and A. A. Kobrinsky 1973 *Vibroimpact Systems* (in Russian) Moscow: Nauka.
18. Ya. G. Panovko 1977 *Introduction to the Theory of Mechanical Impact*. Moscow: Nauka.
19. V. I. Babitsky 1978 *Theory of Vibroimpact Systems* (in Russian) Moscow: Nauka.
20. J. A. Zukas 1982 *Impact Dynamics*. New York: John Wiley.
21. R. M. Brach 1991 *Mechanical Impact Dynamics*. New York: John Wiley.
22. V. Ph. Zhuravlev 1977 *Izvestiva AN SSSR Mekhanika Tverdogo Tela (Mechanics of Solids)* **12**, 24–28. Investigation of certain vibro-impact systems by the method of nonsmooth transformations.
23. V. N. Pilipchuk 1985 *Pricladnaya Matematika Mekhanika (PMM)* **49**, 572–578. The calculation of strongly non-linear systems close to vibration impact systems.
24. V. N. Pilipchuk 1988 *Doklady AN UkrSSR (Ukrainian Academy of Sciences Reports)* **A**(4), 37–40. A transformation of vibrating systems based on a non-smooth periodic pair of functions.
25. V. N. Pilipchuk 1996 *Journal of Sound and Vibration* **192**, 43–64. Analytical study of vibrating systems with strong non-linearities by employing saw-tooth time transformations.
26. A. F. Vakakis, L. I. Manevitch, Yu. V. Mikhlin, V. N. Pilipchuk and A. A. Zevin 1996 *Normal Modes and Localization in Non-linear Systems*. New York: Wiley-Interscience.
27. J. Shaw and S. W. Shaw 1989 *Transactions of the American Society of Mechanical Engineers*, *Journal of Applied Mechanics* **46**, 168–174. The onset of chaos in a two-degree-of-freedom impacting system.
28. K. H. Hunt and F. R. E. Grossley 1975 *Transactions of the American Society of Mechanical Engineers*, *Journal of Applied Mechanics* **97**, 440–445. Coefficient of restitution interpreted as damping in vibroimpact.
29. E. G. Vedenova, L. I. Manevich and V. N. Pilipchuk 1985 *Pricladnaya Matematika Mekhanika* (*PMM*) **49**(2), 153–159. Normal oscillations of a string with concentrated masses on nonlinear supports.